

by earthquake attack can be classified as sliding failure, liquefaction failure, longitudinal cracks, transverse cracks, and piping failure (Chen, 1995). Numerical computation based on constitutive model of geotechnical materials is one of the effective ways to conduct seismic analyses and seismic safety assessment.

5 Earth dams are complicated nonhomogeneous geotechnical structures composed of different materials such as rockfill and clayey soils. This results in great difficulty to analyse and predict the responses of earth dams under various conditions, such as construction, reservoir impounding and earthquake attacks (Costa and Alonso, 2009; Seo and Ha, 2009). Therefore, existing theories and numerical analyses of earth-rockfill
10 dams include many simplifying assumptions (Prevost et al., 1985).

Pseudo static method (Seed and Martin, 1966) is largely used in the numerical analyses to assess the seismic response of earth dams. In this approach, seismic effect on dam body is considered with an equivalent static force, which is the product of soil mass multiplied by a seismic coefficient, and soil is assumed as rigid-perfectly plastic
15 behaving.

Newmark (Newmark, 1965) presented the important concept that the seismic stability of slopes is more important rather than the traditional factor of safety, and he proposed a double integration method to compute the permanent displacement under cyclic loading, which is based on the concept of analyses of a rigid block sliding on
20 a plane. Once the acceleration exceeds the "yield acceleration", permanent displacement can be obtained by double integrating the acceleration.

Up to now, most numerical earthquake response analyses of earth-rockfill dams were conducted using equivalent linear models, in which shear modulus and damping ratio are obtained by iterative procedure (Abdel-Ghaffar and Scott, 1979; Mejia et al.,
25 1982). Cascone and Rampello (2003) evaluated the seismic stability of an earth dam via the decoupled displacement analysis to compute the earthquake-induced displacements.

Parish et al. (2009) performed a study of the seismic response of a simplified typical earth dam using the FLAC3D software. Non-associated Mohr–Coulomb criterion was

2321

adopted to describe the behaviour of both shells and core of the earth dam. Their analyses showed that plasticity should be considered in the analysis of the seismic response of the dam, as it leads to a decrease in the natural frequency of the dam, which could significantly affect the seismic response of the dam. However, this study
5 did not consider the fluid-skeleton interaction, which should have a significant influence on the seismic response of earth dams.

Siyahi and Arslan (2008) studied the dynamic behaviour and earthquake resistance of Alibey earth dam located in Turkey by adopting the OpenSees software (Open System for Earthquake Engineering Simulation) (2000). Elastoplastic constitutive models
10 of soils such as pressure dependent and independent multi-yield materials were implemented in the analyses. They obtained the permanent displacements and concluded that the liquefaction effect is not significant.

However, so far, application of solid-fluid coupled elasto-plastic dynamic analyses in safety assessment of earth-rockfill dams is not much. Furthermore, the initial stress field needed for dynamic computation is often provided without considering the effects
15 of early construction and reservoir impounding.

In this work, the static and dynamic responses of Nuozhadu high earth-rockfill dam have been studied by solid-fluid coupled nonlinear method, since solid-fluid interaction has a significant influence on the behaviour of earth dams. First, the dam site and
20 detailed design data are introduced. The adopted numerical analysis method and soil constitutive model parameters are presented.

In the static analysis, the practical construction was simulated. Then, reservoir impounding was simulated by conducting solid-fluid coupled analysis.

At last, the coupled nonlinear dynamic analyses were conducted based on the initial stress field obtained from the preceding computation. The acceleration component of
25 the El Centro 1940 earthquake was chosen as seismic motion. The excess pore water pressure, acceleration responding, and permanent displacements induced by seismic move are presented and analysed.

2322

Acknowledgements. This work was supported by National Nature Science Foundation of China (51179092) and State Key Laboratory of Hydroscience and Engineering Project (2012-KY-02 and 2013-KY-4).

References

- 5 Abdel-Ghaffar, A. M. and Scott, R. F.: Shear moduli and damping factors of earth dam, *J. Geotech. Geoenviron.*, 105, 1405–1426, 1979.
- Cascone, E. and Rampello, S.: Decoupled seismic analysis of an earth dam, *Soil Dyn. Earthq. Eng.*, 23, 349–365, 2003.
- Chen, M.: Response of an earth dam to spatially varying earthquake ground motion, Ph. D. Dissertation, Civil and Environmental Engineering, Michigan State University, USA, 1995.
- 10 Costa, L. and Alonso, E.: Predicting the behavior of an earth and rockfill dam under construction, *J. Geotech. Geoenviron.*, 135, 851–862, 2009.
- Finn, W. D., Lee, K. W., and Martin, G. R.: An effective stress model for liquefaction, *Electron. Lett.*, 103, 517–533, 1977.
- 15 Gazetas, G.: Seismic response of earth dams: some recent developments, *Soil Dyn. Earthq. Eng.*, 6, 2–47, 1987.
- Hunter, G. and Fell, R.: Rockfill modulus and settlement of concrete face rockfill dams, *J. Geotech. Geoenviron.*, 129, 909–917, 2003.
- Itasca Consulting Group, Inc: FLAC (Fast Lagrangian Analysis of Continua), Version 3.0., Minneapolis, MN, 2005.
- 20 McKenna, F., Fenves, G. L., and Scott, M. H.: Open system for earthquake engineering simulation, Univ. of California, Berkeley, Calif, USA, 2000.
- Mejia, L. H., Seed, H. B., and Lysmer, J.: Dynamic analysis of earth dams in three dimensions, *J. Geotech. Eng-ASCE*, 108, 1586–1604, 1982.
- 25 Newmark, N. M.: Effects of earthquakes on dams and embankments, *Geotechnique*, 15, 139–160, 1965.
- Parish, Y., Sadek, M., and Shahrour, I.: Review Article: Numerical analysis of the seismic behaviour of earth dam, *Nat. Hazards Earth Syst. Sci.*, 9, 451–458, doi:10.5194/nhess-9-451-2009, 2009.

2331

- Prevost, J. H., Abdel-Ghaffar, A. M., and Lacy, S. J.: Nonlinear dynamic analyses of an earth dam, *J. Geotech. Eng-ASCE*, 111, 882–897, 1985.
- Seed, H. B.: Earthquake-resistant design of earth dams, *Can. Geotech. J.*, 4, 1–27, 1967.
- Seed, H. B. and Martin, G. R.: The seismic coefficient in earth dam design, *J. Soil Mech. Found. Div.*, 92, 25–58, 1966.
- 5 Seo, M. W. and Ha, I. S.: Behavior of concrete-faced rockfill dams during initial impoundment, *J. Geotech. Geoenviron.*, 135, 1070–1081, 2009.
- Siyahi, B. and Arslan, H.: Nonlinear dynamic finite element simulation of Alibey earth dam, *Environ. Geol.*, 54, 77–85, 2008.
- 10 Soroush, A. and Jannatiaghdam, R.: Behavior of rockfill materials in triaxial compression testing, *Int. J. Civil Eng.*, 10, 153–161, 2012.
- Yasuda, N. and Matsumoto, N.: Dynamic deformation characteristics of sands and rockfill materials, *Can. Geotech. J.*, 30, 747–757, 1993.

2332

Table 1. Material properties of earth dam soils.

	Units	RD1/RU1	RD2/RU2	RD3/RU3	F1	F2	Clay
Dry density	kg m ⁻³	2190	2310	2170	2000	2050	2120
Young's modulus	MPa	100	100	100	80	80	25
Poisson's ratio	–	0.3	0.3	0.3	0.3	0.3	0.3
Cohesion	kPa	141	114	106	127	105	73
Friction angle	Degree	40.8	39.0	42.8	40.2	39.4	27.1
Dilation angle	Degree	15.8	14.0	17.8	15.2	14.4	12.1
Permeability coefficient	cm s ⁻¹	1.0 × 10 ⁻¹	1.0 × 10 ⁻¹	1.0 × 10 ⁻¹	1.0 × 10 ⁻¹	1.0 × 10 ⁻¹	1.0 × 10 ⁻⁶

2333

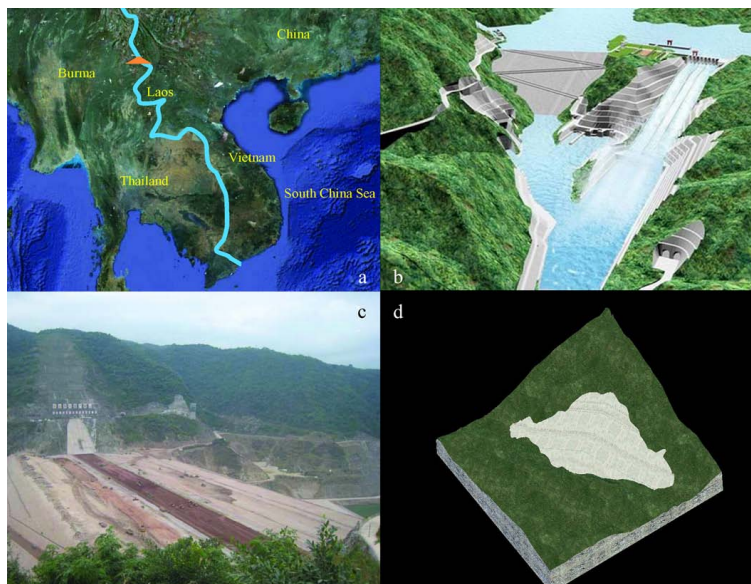


Fig. 1. Nuozhadu dam. **(a)** Nuozhadu dam location, **(b)** Project blueprint, **(c)** Nuozhadu dam under construction, **(d)** Dam site geomorphology.

2334

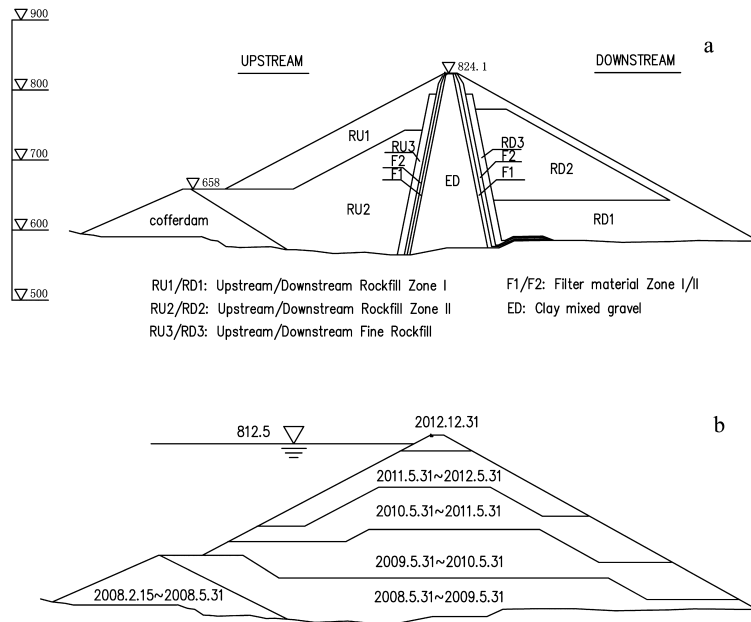


Fig. 2. Maximum cross section with material zoning and construction stage.

2335

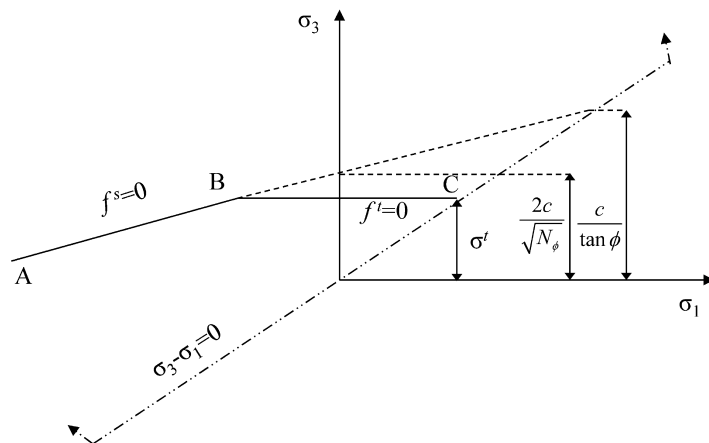


Fig. 3. Mohr-Coulomb failure criterion.

2336

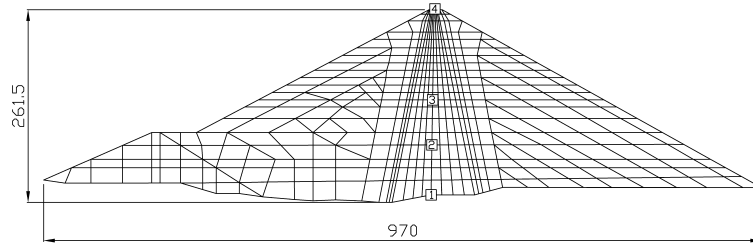


Fig. 4. Numerical mesh and monitoring points (m).

2337

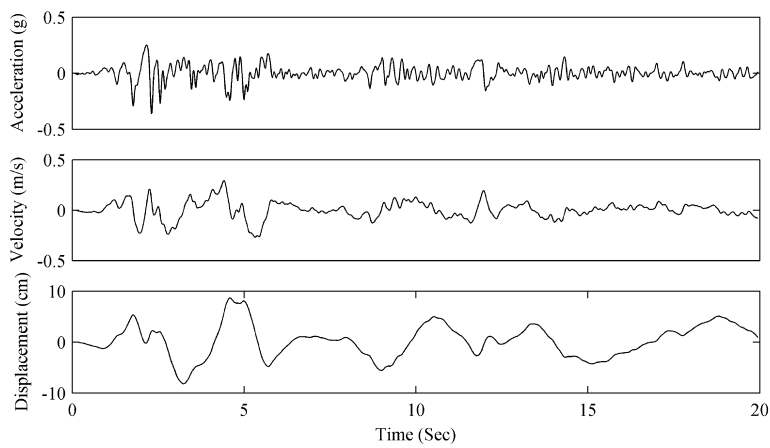


Fig. 5. Seismic wave time history.

2338

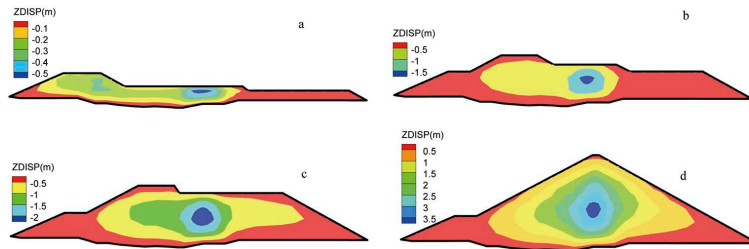


Fig. 6. Construction stages with settlements. **(a)** Stage 10, **(b)** Stage 20, **(c)** Stage 30, **(d)** Stage 45.

2339

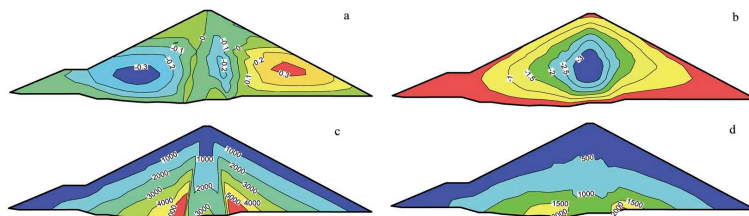


Fig. 7. Contour lines of displacements and principle stresses. **(a)** Horizontal displacement (m), **(b)** Vertical displacement (m), **(c)** Major principle stress (kPa), **(d)** Minor principle stress (kPa).

2340

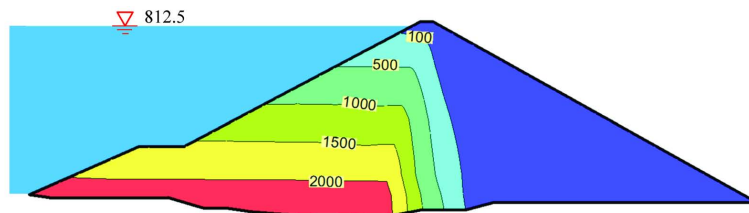


Fig. 8. Reservoir water level and contour lines of pore water pressure (kPa).

2341

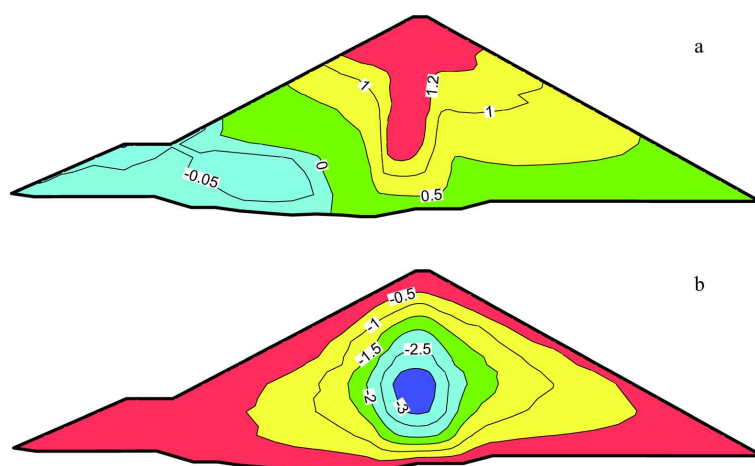


Fig. 9. Contour lines of displacements. **(a)** Horizontal displacement (m), **(b)** Vertical displacement (m).

2342

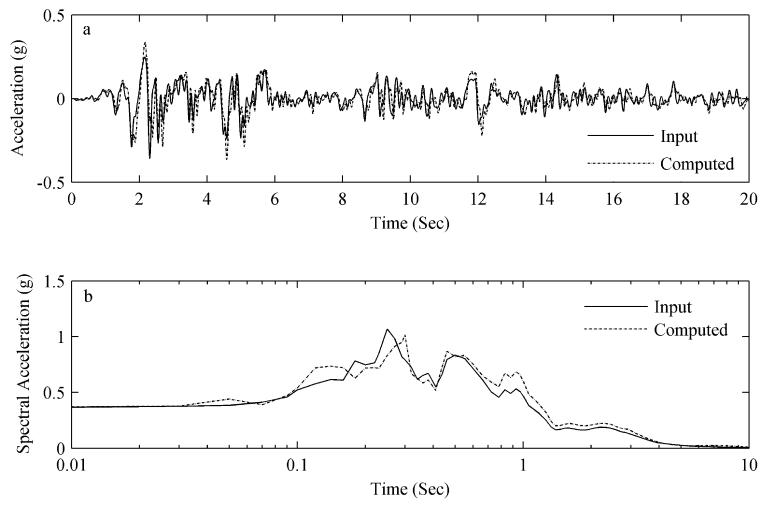


Fig. 10. Acceleration and spectral. **(a)** Acceleration, **(b)** Acceleration response spectral.

2343

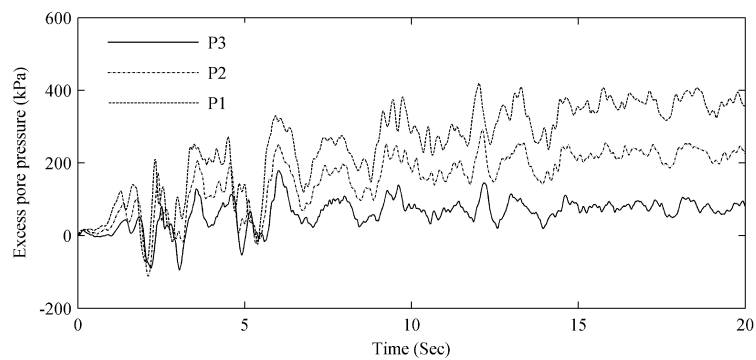


Fig. 11. Excess pore water pressure in different elevations.

2344

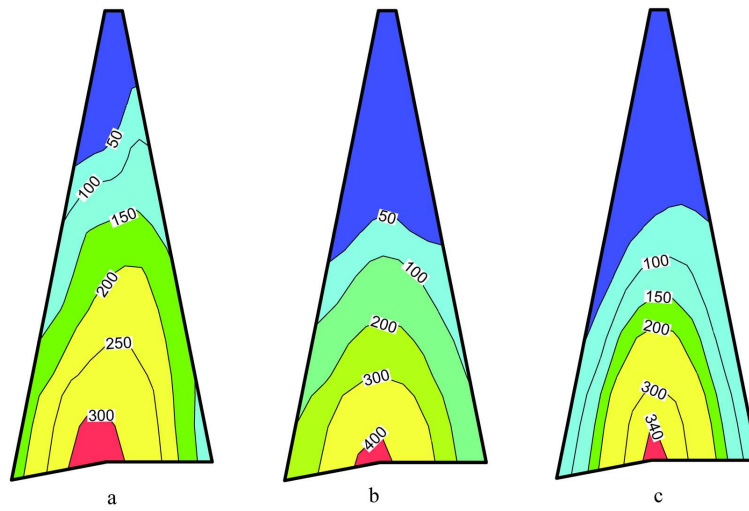


Fig. 12. Distribution of excess pore water pressure in the earth core at different times. **(a)** At 6 s, **(b)** at 12 s, **(c)** at 20 s.

2345

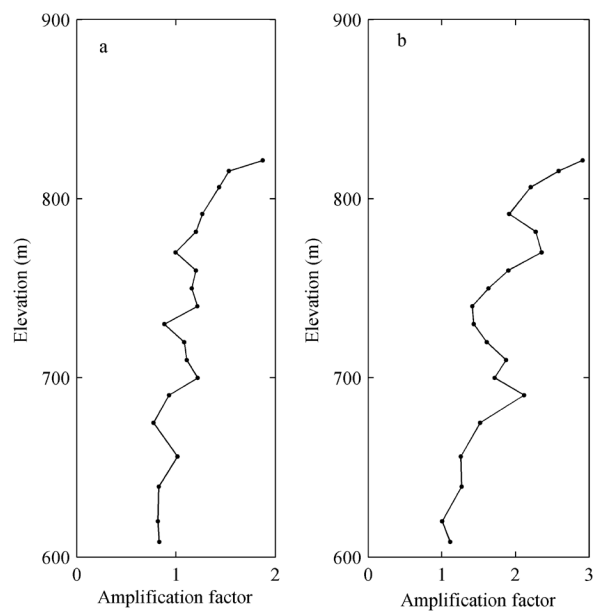


Fig. 13. Acceleration amplification. **(a)** Horizontal, **(b)** vertical.

2346

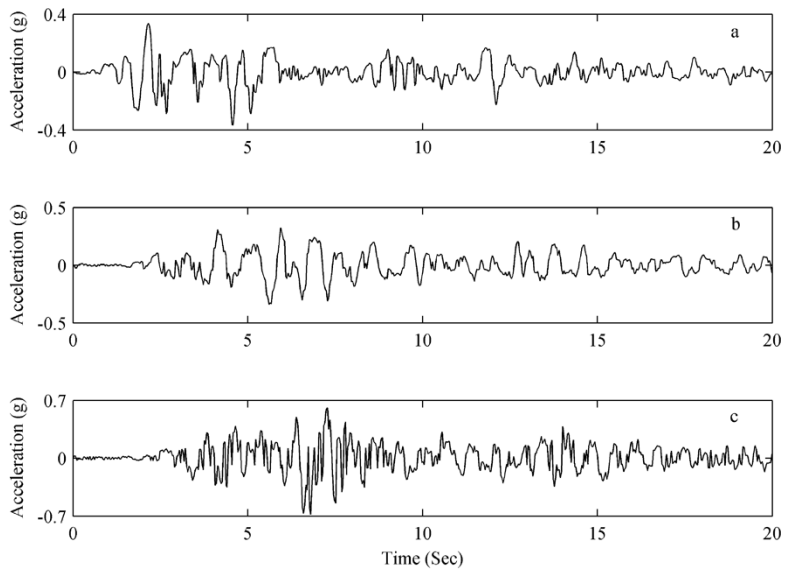


Fig. 14. Horizontal acceleration time history. **(a)** P1, **(b)** P3, **(c)** P4.

2347

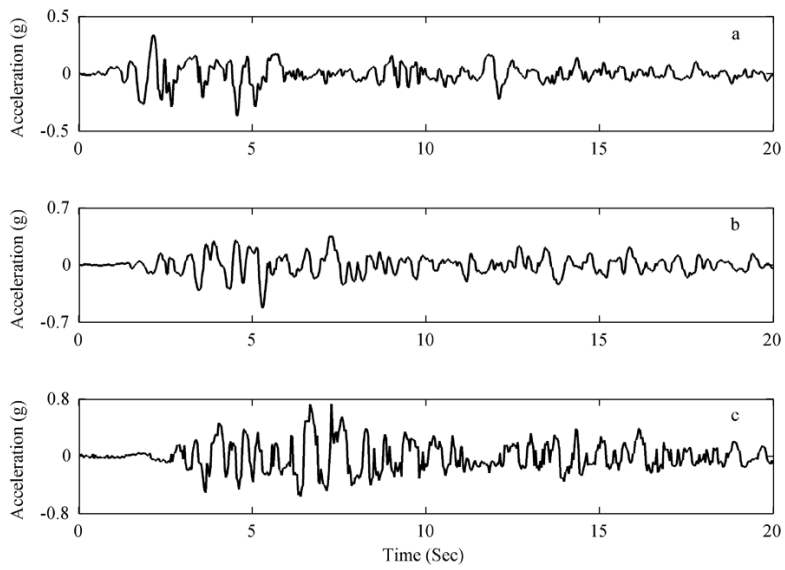


Fig. 15. Vertical acceleration time history. **(a)** P1, **(b)** P3, **(c)** P4.

2348

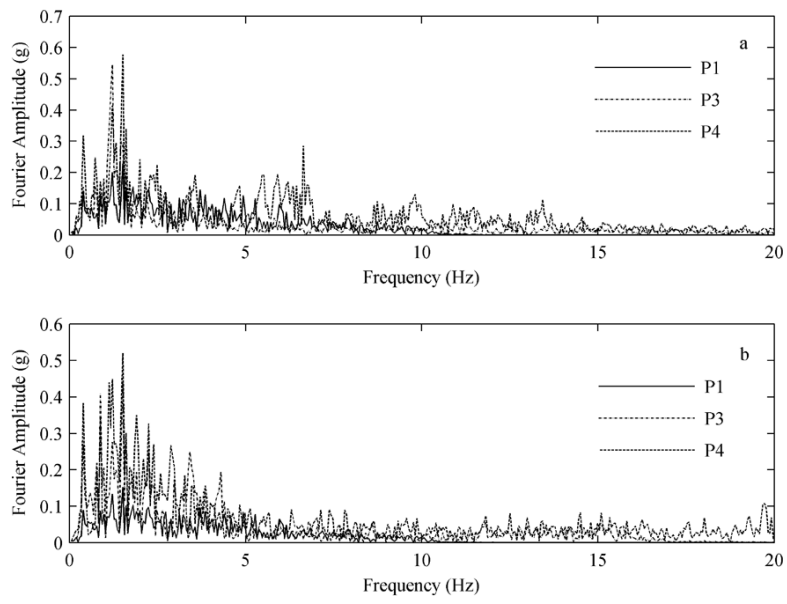


Fig. 16. Fourier spectrum of acceleration. **(a)** Horizontal, **(b)** vertical.

2349

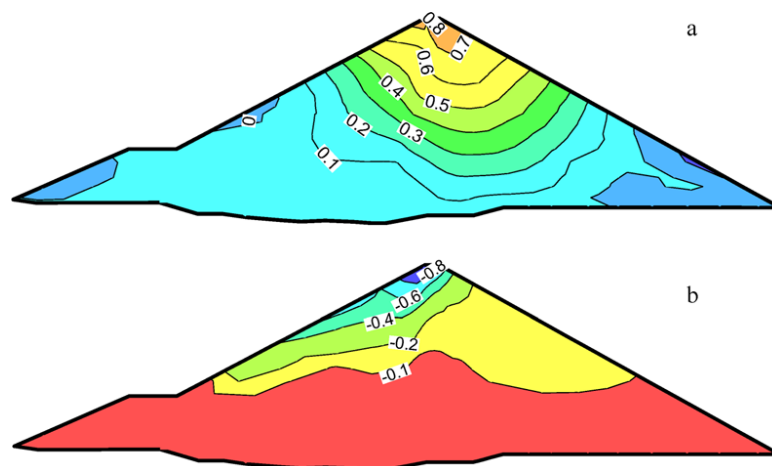


Fig. 17. Contour lines of permanent displacements. **(a)** Horizontal displacement (m), **(b)** vertical displacement (m).

2350

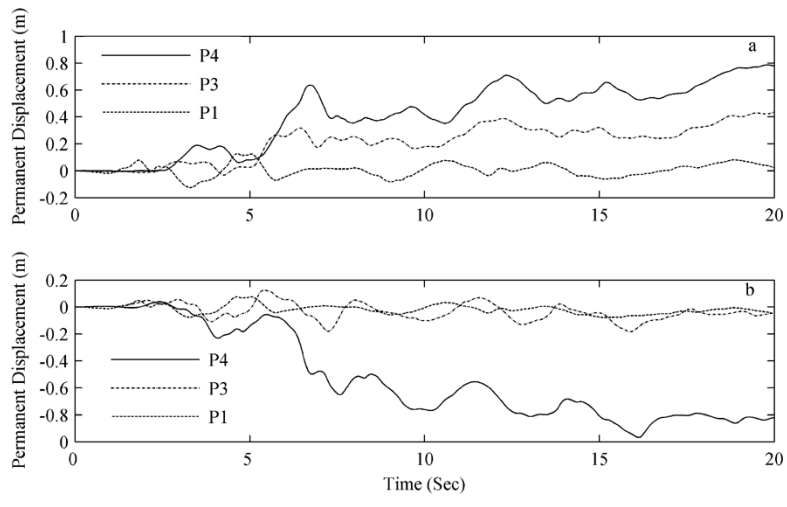


Fig. 18. Displacement time history at different elevations in the core center. **(a)** Horizontal, **(b)** vertical.